

# Robust Estimation and Control of Body Slip Angle for Electric Vehicle

Yoshifumi Aoki, Yoichi Hori

## Abstract

Electric Vehicles (EVs) are inherently more suitable for active safety, which means to control body slip angle  $\beta$  and yaw rate  $\gamma$ , than Combustion engine Vehicles. However as  $\beta$  is difficult to measure, we need to estimate  $\beta$ . We proposed a novel method to estimate  $\beta$ . We did experiments by using UOT March II and their results demonstrated that the proposed observer could estimate  $\beta$  exactly and robustly. Next, we proposed new control methods for 2-Dimension control. We tried to decoupled and control  $\beta$  and  $\gamma$  by feedback and feedforward controller. Simulation results are shown to verify the effectiveness of the proposed method.

**Keywords:** Safety, Controller, EV (electric vehicle).

## 1 Introduction

Recently, Electric Vehicles (EVs) become more popular thanks to the dramatic improvement of motors' and batteries' performances. Most of people like EVs because they think EVs are easy on the environment and can solve today's energy problems.

However, it is not well recognized that EVs have other advantages over Internal Combustion engine Vehicles (ICVs) [1]. Those advantages can be summarized in three aspects.

First, motor's torque generation is fast and accurate. Electric motor's torque response is only several milliseconds, which is 10-100 times as fast as combustion engine's. This advantage can enable us to realize high performance control of EVs. Precise and high speed control is possible for EVs. Because electric motors can be controlled much more precisely, with a shorter control period than ICVs'.

Second, motor torque can be known precisely. Therefore we can easily estimate driving and braking forces between tire and road surface in real-time. This advantage can be used to realize novel control based on road condition.

Third, in-wheel motors can be installed in EVs' each rear and front tires. We can control each torques of the four motors so that it is easier to control EVs' slip angle  $\beta$  and yaw rate  $\gamma$  than ICVs'. In order to make full use of EVs' advantages, it is essentially important to research on  $\beta$  and  $\gamma$  control and  $\beta$  observer. Control diagram is Fig.1.

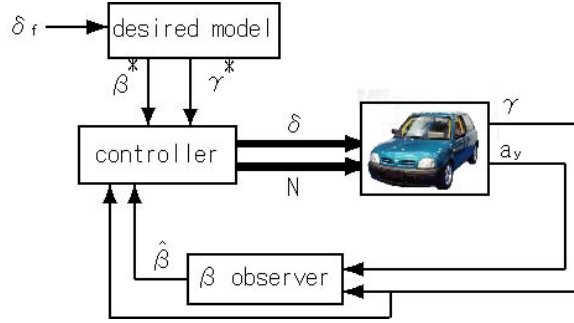


Fig. 1: the full picture of the proposed control method

In order to estimate  $\beta$ , we utilize full order linear observer because nonlinear observer is too complex to control  $\beta$  and  $\gamma$ . We design observer's gain matrix and propose a new method based on  $\gamma$  and side acceleration  $a_y$ . We did experiments by using UOT March II. Experiments show the proposed observer can estimate  $\beta$  accurately and the observer is robust against parameter variation.

Next, we try to control  $\beta$  and  $\gamma$ . If  $\beta$  and  $\gamma$  can be decoupled and controlled freely, EVs movements will be dramatically improved. We design the decoupled controller by using feedback and feedforward controller and utilize Model Following Control (MFC). Simulation results are shown to verify the effectiveness of the proposed method.

## 2 Modeling of EVs

For the proposed observer and controller design, two-wheel model [2] (Fig.2) is used. Generally, in order to describe vehicle's two dimension movement exactly, four-wheel model is needed. However because four-wheel model is non-linear model, it cannot be used for linear observer design.

P is the center of gravity,  $l_f$  is the distance from P to the front wheel,  $l_r$  is the distance from P to the rear wheel,  $\alpha_f$  is the front wheel slip angle,  $\alpha_r$  is the rear wheel slip angle and  $\delta_f$  is actual steering angle at tire.

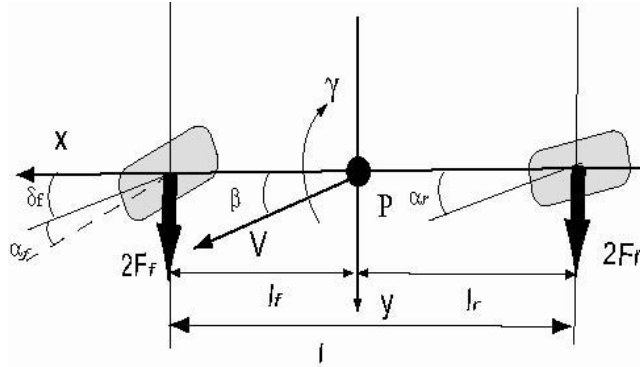


Fig.2: two-wheel model of vehicle motion

Usually, we express state equations with  $\beta$ ,  $\gamma$ , and vehicle speed  $v$ , which are expressed in Equ. (1).

$$\dot{x} = Ax + Bu \dots (1)$$

$$A = \begin{pmatrix} \frac{-2(C_f + C_r)}{mv} & \frac{-2(l_f C_f - l_r C_r)}{mv^2} - 1 \\ \frac{-2(l_f C_f - l_r C_r)}{I} & \frac{-2(l_f C_f^2 + l_r C_r^2)}{Iv} \end{pmatrix}, \quad B = \begin{pmatrix} \frac{2C_f}{I} & 0 \\ \frac{2l_f C_f}{I} & \frac{1}{I} \end{pmatrix}, \quad x = \begin{pmatrix} \beta \\ \gamma \end{pmatrix}, \quad u = \begin{pmatrix} \delta_f \\ N \end{pmatrix}$$

where  $N$  is the yaw-moment which is generated between the left and right drive wheel.  $C_f$  and  $C_r$  are cornering power CP, which is defined as Equ. (2)

$$C_f = \frac{\partial F_{y-f}}{\partial \alpha_f}, \quad C_r = \frac{\partial F_{y-r}}{\partial \alpha_r} \dots (2)$$

where  $F_{y-f}$  and  $F_{y-r}$  are each front and rear wheel's force in  $y$  direction

### 3 Design of the proposed observer

#### 3.1 Restructuring of output equation by using side acceleration $a_y$

Previously, many people proposed many methods for estimating  $\beta$ . For example, in some method [3],  $\beta$  is estimated by Equ. (3). Estimated  $\beta$  by this method contains steady state error, therefore it is not useful. In other method [4], nonlinear observer is used. By using this method, you can estimate  $\beta$  exactly. But due to the complexity of this method, it is not suitable for control.

$$a_y = v(\dot{\beta} + \gamma) \dots (3)$$

Because linear observer's structure is very simple, it is suitable for control. However conventional linear observer is not robust enough against model error and it cannot estimate  $\beta$  exactly in non-linear region.

In this paper, we propose a novel linear observer for estimating  $\beta$ , which can overcome these disadvantages. In conventional linear observers, only  $\gamma$  is used as measurable signal. But in proposed observer,  $a_y$  together with  $\gamma$  are used, which can estimate  $\beta$  in non-linear region [5].

To design the novel observer, it is necessary to restructure output equation,  $a_y$ . Using Eqs. (1) and (3),  $a_y$  can be restructure as:

$$a_y = v(a_{11}\beta + a_{12}\gamma + b_{11}\delta_f + \gamma) \dots (4)$$

where  $a_{11}$  and  $b_{11}$  are each elements of matrix  $A$  and  $B$

Using Eqs. (1) and (4), the output equation is:

$$y = Cx + D\delta_f \dots (5)$$

$$C = \begin{pmatrix} 0 & 1 \\ va_{11} & v(a_{12} + 1) \end{pmatrix}, \quad D = \begin{pmatrix} 0 \\ vb_{11} \end{pmatrix}, \quad y = \begin{pmatrix} a_y \\ \gamma \end{pmatrix} \dots (6)$$

### 3.2 Full order observer

We use full order observer (Fig. 3), which is defined by the following equations.

$$\dot{\hat{x}} = A\hat{x} + Bu - K(\hat{y} - y) \dots (7)$$

$$\hat{y} = Cx + Du \dots (8)$$

where K is observer matrix gain.  $\hat{x}$  is estimated  $x$

The estimation error equation  $e = \hat{\beta} - \beta$  should satisfy the following error equation:

$$\dot{e} = (A - KC)e \dots (9)$$

Full order observer's characteristic is decided by value of matrix gain K.

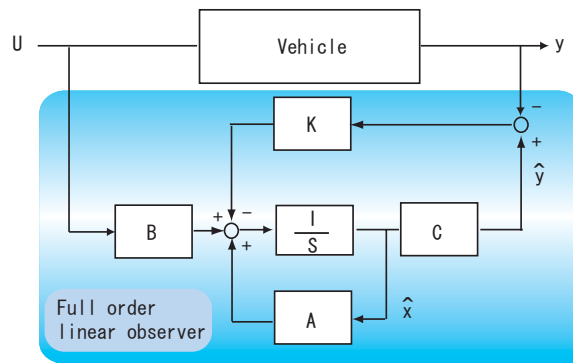


Fig. 3: full order linear observer

### 3.3 Design of gain matrix for robustness

If the selected matrix gain is inadequate, the linear observer will have a poor robust performance against model error and sometimes cannot estimate  $\beta$  exactly. To decide matrix gain, we must consider two important factors.

First, the observer must be designed robust against model error. Since two-wheel model is used in our design, some model error exists more or less. Especially, cornering power  $C_f$  and  $C_r$  depend on road condition and loads on each tires. Therefore, their values are changing and cannot be measured.

Second, all eigenvalues of  $A - KC$  must be located in stable region.  $A - KC$  is the state transition matrix of Equ. (15). The positions of  $A - KC$  eigenvalues will affect control system's time response performances, such as overshoot, rising time and settling time.

To make the observer robust, we referred [6]. By calculate Eqs. (7) and (8), we can get  $\hat{\beta}$ :

$$\dot{\hat{\beta}} = a_{11}\hat{\beta} + a_{12}\hat{\gamma} + b_{11}\delta_f - k_{11}(\hat{\gamma} - \gamma) - k_{12}(\hat{a}_y - a_y) \dots (10)$$

State equation of  $\beta$  is expressed as:

$$\dot{\beta} = a'_{11}\beta + a'_{12}\gamma + b'_{11}\delta_f \dots (11)$$

where  $a'_{11}$ ,  $a'_{12}$  and  $b'_{11}$  are the real values. Any model error is not contained in this equation

By Eqs. (10) and (11), the state equation for  $\hat{\beta} - \beta$  is given by following equation.

$$\begin{aligned} \dot{\hat{\beta}} - \dot{\beta} &= (\hat{\beta} - \beta)(a_{11} - k_{12}v) - (1 - k_{12}v)(a'_{11} - a_{11})\beta \\ &+ (\hat{\gamma} - \gamma)[a_{12} - k_{12}v(a_{12} + 1) - k_{11}] \\ &- (1 - k_{12}v)(a'_{12} - a_{12})\gamma \\ &+ (1 - k_{12}v)(b_{11} - b'_{11})\delta_f \dots (12) \end{aligned}$$

Because we can measure  $\gamma$  by a gyro sensor,  $\hat{\gamma}$  can be assumed to be equal to  $\gamma$ . The best condition for robustness is:

$$1 - k_{12}v = 0 \Leftrightarrow k_{12} = \frac{1}{v} \dots (13)$$

By Equ. (13), Equ. (12) is expressed as:

$$\dot{\hat{\beta}} - \dot{\beta} = (a_{11} - 1)(\hat{\beta} - \beta) \dots (14)$$

Because the eigenvalue of  $a_{11} - 1$  is located in stable region,  $\hat{\beta}$  converges to  $\beta$ .

Matrix gain K is decided as:

$$K = \begin{pmatrix} \frac{\lambda_1 \lambda_2 (l_f - l_r) I}{C_f [2(l_f^2 + l_r^2) + 4l_f l_r]} - 1 & \frac{1}{v} \\ -\lambda_1 - \lambda_2 & \frac{m(l_f^2 + l_r^2)}{(l_f - l_r) I} \end{pmatrix} \dots (15)$$

where  $\lambda_1$  and  $\lambda_2$  are the assigned poles of the observer

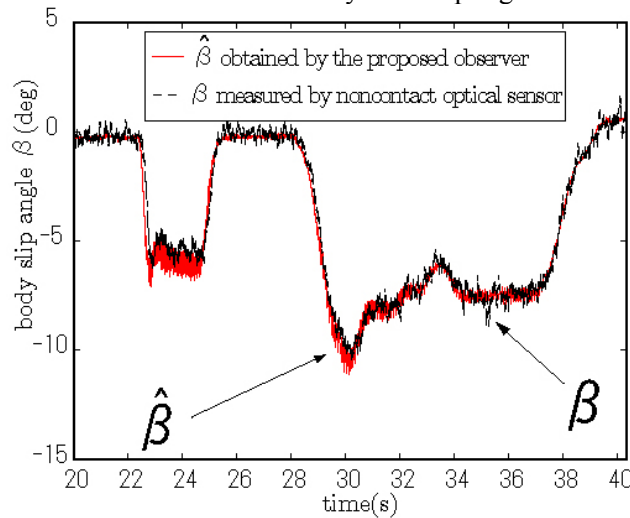
## 4 Experimental demonstrations for the novel observer by UOT March II

### 4.1 Experiment setup for the proposed observer

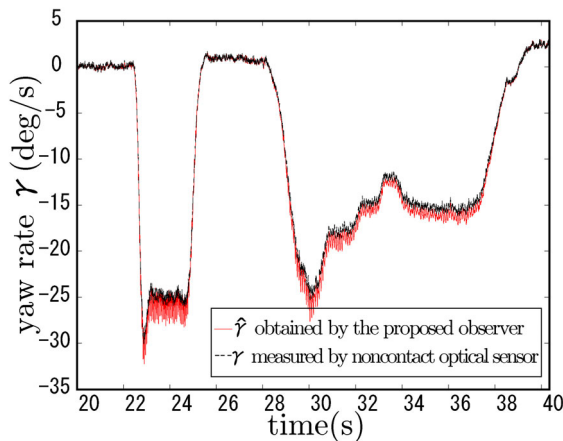
We remodeled Nissan March as our experimental EV, UOT March II built to prove EVs' advantages. Sensors of UOT March II are acceleration sensor, gyro sensor and noncontact speed meter which enable us to measure  $\beta$ . Table. 1 explains specifications.

We did various experiments and two of the experimental results were shown you. Vehicle velocity, driver's input steering wheel angle  $\delta_f$  and road type were changed to test the effectiveness and robustness of the proposed observer. While the experiment was done, road type is changed from dry road to wet road. But observer's parameters are kept unchanged. Steering angle was changed freely by the test driver.

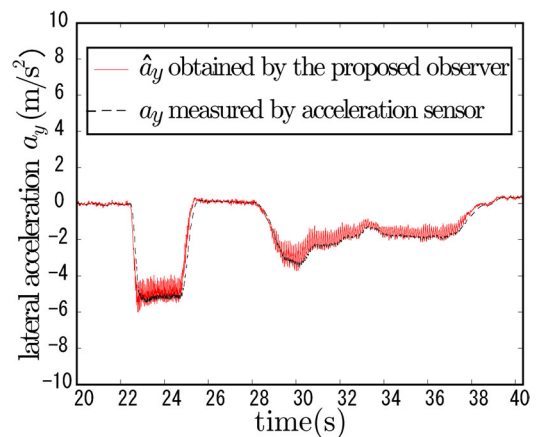
We recorded  $\beta$ ,  $\gamma$ ,  $\delta_f$ ,  $v$  and  $a_y$  in hard disk drive by the sampling time of 1 [ms].



(a) Measured value and estimation of  $\beta$



(b) Measured value and observer's output of  $\gamma$



(c) Measured value and observer's output of  $a_y$

Fig. 4 experimental results for the proposed observer's effectiveness

## 4.2 Experimental results for the proposed observer

Figs. 4 and 5 show the experimental results under the same experiment condition. But observers' condition is difference.

Fig. 4 show the experimental result in nonlinear religion for the effectiveness of the proposed observer. Fig. 4 (a) is measured and estimated  $\beta$ . Fig. 4 (b) and (c) are measured value and observer's output of  $a_y$  and  $\gamma$ . Fig.4 shows us that the novel observer can estimate  $\beta$  exactly and robustly even if road type and cornering power were changed.

In Fig. 5, the two linear observers were used and 70 percent error in  $b_{11}$  intentionally. One observer is the novel observer. The other observer has different matrix gain (see Equ. (16)). Even if the observers have model error, the novel observer can estimate  $\beta$  exactly. But the other observer cannot estimate  $\beta$ . Fig. 5 proves that our design of gain matrix can make the linear observer more robust.

Table 1: Sensors of UOT March II

PC to control	Pentium MMX 223[MHz]
	AMD K6-233[MHz]
OS	Slackware Linux 3.5
	RTLlinux rel. 9K
encoder pulse number	3600[ppr]
Acceleration sensor	ANALOG DEVICES ADXL202
Yaw rate sensor	HITACHI OPTICAL FIBER GYROSCOPE HOFG-CLI(A)
Noncontact Optical sensor	CORREVIT S-400

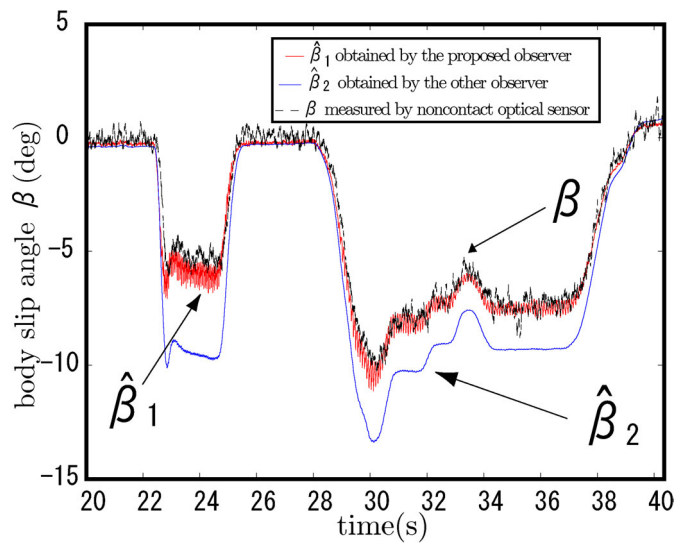


Fig. 5 experimental results for the proposed observer's robustness

$$K = \begin{pmatrix} \frac{\lambda_1(a_{12} + 1)}{a_{11}} - 1 & \frac{a_{11} - \lambda_1}{va_{11}} \\ a_{22} - \frac{a_{21}(a_{12} + 1)}{a_{11}} - \lambda_2 & \frac{a_{21}}{va_{11}} \end{pmatrix} \dots (16)$$

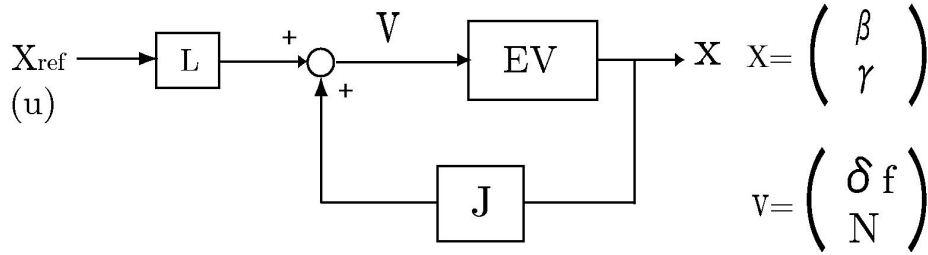


Fig. 6: proposed control diagram

## 5 Proposed controller design

Recently, many researchers study about Active Front Steering system (AFS) and Direct Yaw-moment Control (DYC) [7]. But AFS and DYC interfere each other. AFS and DYC must be designed together and decoupled. We propose a novel method for  $\beta$  and  $\gamma$  controller.

### 5.1 Model Following Control (MFC)

We utilize Model following Control (MFC) in order to generate the reference of the vehicle dynamics, or the “desired” response to driver’s steering input [8]. In this paper, MFC calculates the desired state vector  $x_{ref}$ .

We use linear state equations expressed by Equ. (1) as the desired model. Using Equ. (1),  $x_{ref}$  is:

$$X_{ref} = [sI - A]B \dots (17)$$

where matrix A and B are defined in Equ. (1)

If we can keep the quantities of state  $x$  following the desired value  $x_{ref}$  freely, EVs’ movements and safety will be improved.

### 5.2 Design of decoupling controller

To decouple AFS and DYC, we use feedback controller J and feedforward controller L. Its block diagram is depicted in Fig. (6). Transfer function  $G$  from input  $u$  to state vector  $x$  with the novel controller is given by



$$G = [sI - A - BJ]^{-1} BL = F^{-1} BL \dots (18)$$

where

$$F = sI - A - BJ, \quad G = \begin{pmatrix} G_{11} & G_{12} \\ G_{21} & G_{22} \end{pmatrix}$$

If we can make matrix  $G$  diagonalized, AFS and DYC are decoupled. In this paper, we control  $\beta$  by yaw-moment  $N$  and  $\gamma$  by  $\delta_f$ . Then, the necessary condition for diagonalizing  $G$  is that  $J$  and  $L$  which satisfy Equ. (19) exist.

$$G_{11} = 0, \quad G_{22} = 0, \quad L \neq 0 \dots (19)$$

Calculating Equ. (19), we get the following conditions:

$$l_{11} = 0 \dots (20)$$

$$a_{12} + b_{11}j_{12} = 0 \Leftrightarrow j_{12} = -\frac{a_{12}}{b_{11}} \dots (21)$$

$$l_{12}b_{21} + l_{22}b_{22} = 0 \Leftrightarrow l_{22} = -\frac{b_{22}}{b_{21}}l_{12} \dots (22)$$

$$b_{21}j_{11} + b_{22}j_{21} + a_{21} = 0 \Leftrightarrow j_{21} = -\frac{a_{21} + b_{21}j_{11}}{b_{22}} \dots (23)$$

Additionally considering the condition that steady-state error must be 0,  $L$  and  $J$  are given by:

$$L = \begin{pmatrix} 0 & -\frac{q_1}{b_{11}} \\ -\frac{q_2}{b_{22}} & -\frac{q_1 b_{21}}{b_{22} b_{11}} \end{pmatrix} \dots (24)$$

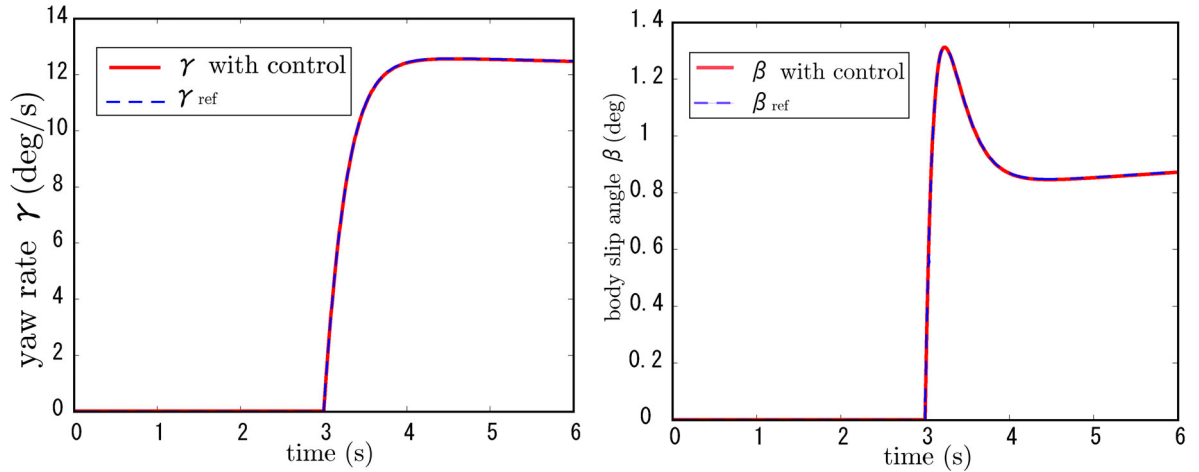
$$J = \begin{pmatrix} \frac{q_1 - a_{11}}{b_{11}} & -\frac{a_{12}}{b_{11}} \\ -\frac{a_{21} b_{11} + b_{21}(q_1 - a_{11})}{b_{11} b_{22}} & \frac{a_{22} b_{21} + b_{11}(q_2 - a_{21})}{b_{11} b_{22}} \end{pmatrix} \dots (25)$$

where  $q_1$  and  $q_2$  are each the assigned poles of  $G_{12}$  and  $G_{21}$

## 6 Simulation results using the proposed controller

This section describes the simulation results of MFC and decoupling control. These simulations were carried out with non-linear formation for vehicle motion.

Fig. 7 shows simulated vehicle motion with the proposed control method. The vehicle dynamics follow “desired model” exactly by the novel control method. In this simulation, actual cornering power  $C_f$  and  $C_r$  are different from their nominal values. Hence, Fig. 7 also shows robustness of the proposed controller against cornering power.

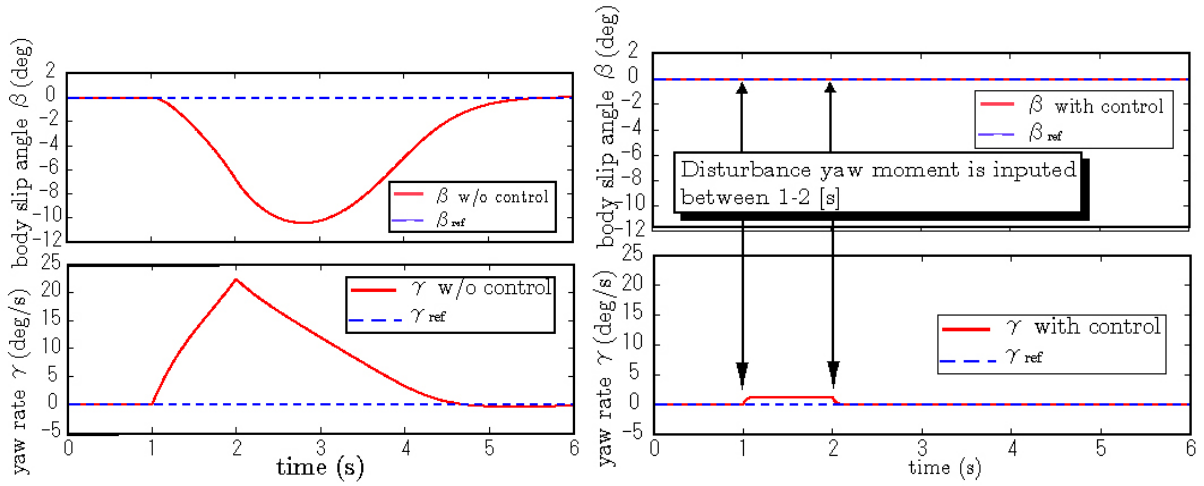


(a) yaw rate with decoupling and MFC control (b) body slip angle with decoupling and MFC control  
Fig. 7: simulation results of the proposed control

Next, we add disturbance yaw moment. Disturbance value is 3000[N] and inputted between 2-3 seconds. This disturbance represents the effects of a sudden gust of wind and etc. In these simulations, the human driver does nothing. Without disturbance, the vehicle would go straight ahead.

Fig. 8 (a) is the simulation result without control. Disturbance makes the vehicle dynamics unwanted value. Fig. 8(b) is the simulation result with control. Even if disturbance exists, the proposed control make vehicle dynamics coincide with the value of the desired response. This figure shows us that the proposed control method is effective against disturbance yaw moment.

Fig.9 presents trajectory of the vehicle. Without the proposed control, the vehicle goes astray. But with the proposed control, the vehicle maintain the course. These results show us that the proposed control can reject disturbances.



(a) vehicle dynamics without decoupling and MFC control  
 (b) vehicle dynamics with decoupling and MFC control  
 Fig. 8: simulation results with disturbance yaw moment 3000[Nm]

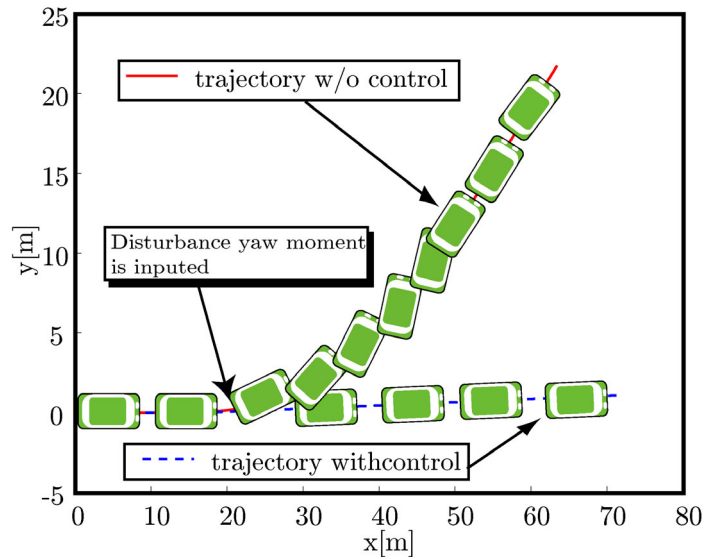


Fig. 9: trajectory of the vehicle with disturbance yaw moment 3000[Nm]

## 7 Conclusion

In this paper, we proposed novel methods to estimate  $\beta$  and to control  $\beta$  for EVs. The improved observer is based on acceleration and yaw rate  $\gamma$  sensors. By this method, we can estimate  $\beta$  robustly and accurately. The results of experiments by using UOT March II demonstrated that the proposed observer could estimate  $\beta$  exactly and robustly. Next, We utilize MFC, feedback and feedforward control method for EVs' motion control.  $\beta$  and  $\gamma$  could be decoupled and  $\hat{x}$  could converge to  $x$  by this control method. Simulation results are shown to verify the effectiveness of the proposed method. In the future, EVs will become more popular and contribute to solving energy problems. It is essential to pursue the researches on making full use of pure EVs' advantages.

## References

- [1] Yoichi Hori: "Future Vehicle driven by Electricity and Control -Research on 4 Wheel Motored 'UOT March II'", AMC 2002, pp.1-14, 2002.
- [2] M. Abe: "Vehicle Dynamics and Control", Sankaido, 1992. (in Japanese)
- [3] Masugi Kaminaga and Genpei Naito: "Vehicles Body Slip Angle Estimation Using an Adaptive Observer", Proceedings of AV EC\_98, 1998.
- [4] Joanny Stephant, Ali Charara and Dominique Meizel: "Virtual Sensor: Application to Vehicle Sideslip Angle and Transversal Forces" IEEE trans. on Industrial Electronics, vol.51, No.2 April 2004
- [5] T. Inoue and Y. Hori: "Observer Design of Drift Angle for Future Vehicle Control and Experimental Evaluation using the Four-Motored Electric Vehicle", EV S -20, 2003.
- [6] Y. Hori and T. Umeno: "Implementation of Robust Flux Observer Based Field Orientation (FOFO) Controller for Induction Machines", 1989 IAS Meeting, pp.523-528, 1989.
- [7] Motoki Shino Masao Nagai.: "Independent wheel torque control of small-scale electric vehicle for handling and stability improvement", JSAE Review, Vol24, No4, 2003, pp.449-456
- [8] Shin-ichiro Sakai and Y. Hori: "Robustified model matching control for motion control of electric vehicle", In Proc. 5<sup>th</sup> Advance Motion Control, pp. 574-579, Coimbra, 1998.

## Author



Yoshifumi Aoki, The Department of Electrical Engineering the University of Tokyo, 7-3-1 Hongo Bunkyo-ku Tokyo 113-8656, Japan  
Tel +03 5452 6289, fax +03 5452 6288, e-mail y-aoki@horilab.iis.u-tokyo.ac.jp

He received academic degree in Electrical Engineering from the University of Tokyo in 2004. He is now 1th-year master's degree student at the University of Tokyo and studies about EVs' motion control.



Yoichi Hori, The Institute of Industrial Science the University of Tokyo, 4-6-1 Komaba Meguro-ku Tokyo 153-8505, Japan  
Tel: +03 5452 6289, Fax: +03 5452 6288, e-mail: hori@iis.u-tokyo.ac.jp,

He received Ph.D degrees in Electrical Engineering from the University of Tokyo in 1983 and joined the Department of Electrical Engineering as a Research Associate. He later became a Professor in 2000. In 2002, he moved to the Institute of Industrial Science as a Professor of Information & Electronics Division. His research fields are control theory and its industrial application to motion control, mechatronics, robotics, electric vehicle, etc. He worked as Treasurer of IEEE Japan Council and Tokyo Section during 2001-2002. He is now the Vice President of IEE-Japan IAS. He is the program chairperson of the coming EVS-22 to be held in Yokohama, October 2006. IEEE Fellow.